

Using B-spline frames to approximate solutions of acoustic scattering problems

Wolfgang Kreuzer^a

^a*Acoustics Research Institute, Austrian Academy of Sciences,
Wohllebengasse 12-14, Vienna, 1040, Vienna*

Abstract

Although frames, which are a generalization of bases, are important tools used in signal processing, their potential in other fields of acoustics has not been fully explored yet. Gabor frames are very well adapted to represent oscillating functions, and therefore have a great potential as ansatz functions for Helmholtz FEM/BEM. In this paper representations of the solution of a scattering problem in 2D using Gabor frames based on B-splines as building blocks are investigated and some properties of these frames will be shown based on numerical experiments.

Keywords: BEM, frames, B-splines

1. Introduction

Numerical methods like the boundary element method (BEM) or finite elements (FEM) play an important role for calculating the scattering of acoustic waves from complex structures, thus for solving the Helmholtz equation (cf. [1, 2, 3, 4]). To that end, the scatterer (or its surface) is discretized with simple geometric elements and based on this discretization the unknown solution $u(\mathbf{x})$ (i.e. the acoustic pressure, the velocity potential or the particle velocity) is represented/approximated using simple (basis) functions: $u(\mathbf{x}) = \sum_{n=0}^N u_n \phi_n(\mathbf{x})$. In general, for Helmholtz problems with uniform grids the number of necessary ansatz functions N is dependent on the wavenumber k (cf. [5, 6]). For high frequencies the computational effort for calculating BEM (or FEM) solutions becomes very large, and calculations of wave scattering problems can last between hours to several days on modern computers.

One idea to circumvent the six-to-eight-elements-per-wavelength rule of thumb in BEM is to include oscillating components in the ansatz functions (e.g. see [7, 8]). As the construction of a basis with special properties can be cumbersome sometimes, ansatz functions based on *Gabor frames* [9, 10, 11, 12], i.e. functions of the type $\phi_{m,n}(x) = g(x - na)e^{2\pi i m b x}$, $m, n \in \mathbb{Z}$, will be used in this work. Frames are generalizations of (bi-orthogonal) bases and, contrary to a basis, lead to redundant representations. Because of the gained freedom/relaxed requirements it is easier to construct frames with special a-priori properties compared to finding appropriate bases (for a hands-on survey on frames and redundancy cf. [13, 14]). A motivation for the advantage of using a (redundant) frame instead of a basis can be given by the following example: In a “rich” dictionary with a lot of entries, it is much easier to find the correct pieces to have a short, i.e. sparse, representation of a given sentence.

Similar to Riesz bases, frames allow to represent arbitrary elements of the Hilbert space by series expansions with respect to the frame elements. Frames have already found some application in signal processing [15, 16] and psychoacoustics [17, 18].

In this paper the idea of using frames for approximating solutions of scattering problems is presented. There is already some literature in connection with frames and operator equations, e.g. [19, 20, 21, 22, 23], but most papers are rather on a theoretical and conceptional level. This manuscript aims at a more practical and applied viewpoint of this topic. Some aspects of implementing and applying frames are discussed, and numerical experiments for two different wavenumbers are performed. In this paper, the problems discussed are restricted to 2D scattering problems, however, the extension to higher dimensions is straight forward by using tensor products of one-dimensional frames. It is clear, that for solving 2D scattering problems already very efficient methods exist (e.g. spectral methods based on

Email address: wolfgang.kreuzer@oeaw.ac.at (Wolfgang Kreuzer)

Nyström methods [24]), however, in this paper the focus lies on investigating the potential that frames offer outside the area of signal processing especially with respect to providing efficient representations of oscillating solutions of scattering problems. In that respect, this manuscript should be seen as one of the first steps towards efficient methods for solving 3D scattering problems with relatively large wavenumbers. The main aim of this manuscript is to introduce the concept of frames to the field of applied sciences away from signal processing and to address the question: “*Can Gabor frames be used to provide an efficient representation for solutions of scattering problems?*”.

The paper is structured as follows. In Section 2 a brief overview of B-spline functions, that will play the role as generating window for the Gabor frames, is given. In Section 3 the definition of (Gabor)frames and their duals is given and some of their properties are discussed, especially in connection with Gabor frames based on B-splines as generating window functions. Section 4 deals with practical aspects for implementing frames, e.g. strategies for sampling and ways to calculate the expansion coefficients for arbitrary functions in $L^2(\mathbb{R})$. In Section 5 numerical experiments dealing with the representation of the solution of a scattering problem in 2D using B-spline Gabor frames will be performed. As efficient (sparse) representations will be of interest, some focus will be on the orthogonal matching pursuit algorithm in connection with calculating the unknown frame coefficients.

The octave scripts used in the numerical experiments can be found at <https://www.kfs.oeaw.ac.at/research/projects/biotop/Bsplineframes.tgz>, for a description of the different scripts please refer to the file README.txt in the tar-ball.

2. B-splines

B-spline functions play an important role in numerical mathematics (e.g. as ansatz functions in FEM and BEM or in connection with NURBS curves and isogeometric analysis [25, 26]) and especially in computer graphics (e.g. [27, 28, 29]). They can be easily constructed via

$$N_1(x) = \begin{cases} 1, & x \in [0, 1], \\ 0 & \text{otherwise,} \end{cases} \quad (1)$$

$$N_{\ell+1}(x) = (N_\ell * N_1)(x) = \int_0^1 N_\ell(x-t)dt, \quad (2)$$

where ‘*’ denotes the convolution, for examples please refer to Fig. 1 for the B-splines N_ℓ for orders $\ell = 1, \dots, 4$. Besides their finite support B-splines offer additional interesting properties, e.g.

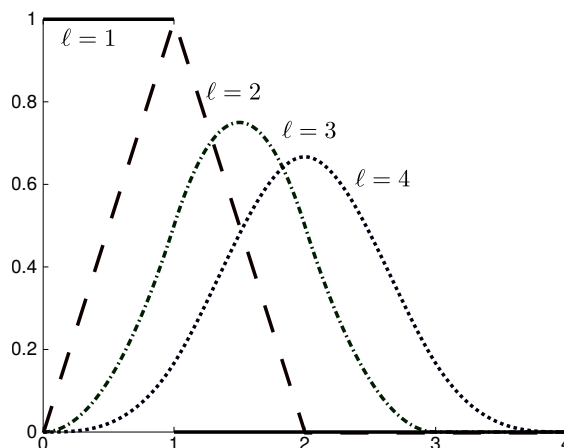


Figure 1: B-splines of order one to four

- $\int_{-\infty}^{\infty} N_\ell(x)dx = 1,$

- partition of unity, i.e. $\sum_{k \in \mathbb{Z}} N_\ell(x - k) = 1$,
- $N_\ell(x) \in C^{\ell-2}(\mathbb{R})$, i.e. N_ℓ is $\ell - 2$ times continuously differentiable,
- N_ℓ restricted to $[k, k + 1]$ is a polynomial of degree at most $\ell - 1$ for all $k \in \mathbb{Z}$,
- $N_\ell(\cdot + k)$, $k = 0, \dots, \ell - 1$ are linearly independent on $[0, 1]$,
- $\int_{-\infty}^{\infty} N_\ell(x) f(x) = \int_{[0,1]^\ell} f(x_1 + \dots + x_\ell) d_{x_1} \dots d_{x_\ell}$.

As already mentioned, the linear independence, the partition of unity property and the compact support make (low order) B-splines good candidates for FEM and BEM ansatz functions, and in our case also as generating window functions for Gabor frames.

3. Frames

A countable family of functions $\{g_i\}_{i \in \mathcal{I}}$ in a Hilbert space \mathcal{H} is called *frame* for \mathcal{H} if there exist constants $A, B > 0$ such that

$$A\|f\|^2 \leq \sum_{i \in \mathcal{I}} |\langle f, g_i \rangle|^2 \leq B\|f\|^2, \quad \forall f \in \mathcal{H}, \quad (3)$$

where $\mathcal{I} \subseteq \mathbb{N}$ is some countable index set. $\langle f, g \rangle$ denotes the scalar product in the Hilbert space, e.g. for $f, g \in L^2(\mathbb{R})$ the product is given by $\langle f, g \rangle = \int_{-\infty}^{\infty} f(x)g^*(x)dx$, where $g^*(x)$ denotes the conjugate complex of the function $g(x)$.

The bounds A and B are called *framebounds*, if $A = B$ the frame is called *tight*. Eq. (3) can be seen as the link between the norm/energy of a function and the norm/energy of its representation using frame atoms $g_i(x)$. Eq. (3) ensures that every element in the vector space can be reconstructed in a stable way using the frame atoms, if the frame bounds are close to each other the reconstruction is faster and behaves numerically better.

For every frame $\{g_i\}_{i \in \mathcal{I}}$ there exists at least one *dual* frame $\{\tilde{g}_i\}_{i \in \mathcal{I}}$ such that

$$f(x) = \sum_{i \in \mathcal{I}} \langle f, \tilde{g}_i \rangle g_i(x) = \sum_{i \in \mathcal{I}} \langle f, g_i \rangle \tilde{g}_i(x), \quad (4)$$

where the sums in the above equation converge absolutely. Thus, every element in the Hilbert space can be represented by a weighted (possibly infinite) sum of frame atoms and the coefficients of this representation can be calculated by the inner product of the target function with the dual frame. A frame is similar to a basis, but as frames can have multiple different dual frames the expansion is *not* unique. Amongst all possible dual frames the *canonical dual* frame plays a special role as it can be constructed by inverting the so called *frame operator* $f \rightarrow \sum_{i \in \mathcal{I}} \langle f, g_i \rangle g_i$, which in practice means by taking the pseudo inverse of the matrix containing the sampled frame elements (see also Section 4). For a more detailed introduction to frames please refer for example to [12].

3.1. Gabor frames

Gabor systems $\mathcal{G}(g, a, b)$ are a collection of functions that are constructed by translating and modulating a given window function $g(x)$:

$$g_{mn}(x) = E_{mb} T_{na} g(x) = g(x - na) e^{2\pi i m b x}, \quad (5)$$

where $a, b \in \mathbb{R}^+$ and $m, n \in \mathbb{Z}$. $E_{mb} f(x) = f(x) e^{2\pi i m b x}$ and $T_{na} f(x) = f(x - na)$ define the modulation and the translation operators, respectively. Under certain conditions on the parameters a and b a Gabor system forms a frame. For Gabor frames it is known that some dual frames (especially the canonical dual) also have a Gabor structure, thus the duals can be constructed by translation and modulation of a *dual window* function (c.f. [30, 31]).

A continuous version of a Gabor frame is given by the short time Fourier transform

$$\text{STFT}\{s(t)\}(\tau, \omega) = \int_{-\infty}^{\infty} s(t) g(t - \tau) e^{-i\omega t} dt, \quad (6)$$

where $g(t)$ is a specific window function (e.g. Hanning window). The STFT is essential for the time-frequency representation of signals $s(t)$, e.g. for generating spectrograms and Gabor frames lead to a sampled version of the STFT.

3.2. Gabor frames based on B-splines

Because of their compact support and especially because of their partition of unity property B-splines are easy to use window functions for generating Gabor frames and some of their duals. Based on the theorems given by Christensen [11, 12, 32] conditions for the frame parameters a, b can be found to derive Gabor frames based on B-splines and to construct some duals frames:

Theorem 1. For $\ell \in \mathbb{N}$, the B-spline $N_\ell(x)$ generates Gabor frames for all $(a, b) \in (0, \ell) \times (0, 1/\ell]$.

Theorem 2. For any $\ell \in \mathbb{N}$, and $b \in (0, \frac{1}{2\ell-1}]$, the functions N_ℓ and

$$h_\ell = bN_\ell(x) + 2b \sum_{k=1}^{\ell} N_\ell(x+k) \quad (7)$$

generate dual frames $\{E_{mb}T_n N_\ell\}_{m,n \in \mathbb{Z}}$ and $\{E_{mb}T_n h_\ell\}_{m,n \in \mathbb{Z}}$.

Theorem 3. For any $\ell \in \mathbb{N}$ and $b \in (0, \frac{1}{2\ell-1}]$, the functions N_ℓ and

$$h_\ell(x) = b \sum_{k=-\ell+1}^{\ell-1} N_\ell(x+k) \quad (8)$$

generate dual frames $\{E_{mb}T_n N_\ell\}_{m,n \in \mathbb{Z}}$ and $\{E_{mb}T_n h_\ell\}_{m,n \in \mathbb{Z}}$.

For the proofs please refer to Corollaries 9.1.9 and 9.4.2 in [12] and Corollary 2.46 in [32]. In Fig. 2 the window function $N_2(x)$ and the two dual windows Dual1 and Dual2 (dashed and dotted, respectively) constructed using Eqs. (7) and (8) for $a = 1$ and $b = \frac{1}{3}$ are shown. In Fig. 2 the (numerically determined) canonical dual window is shown with the dash-dotted line.

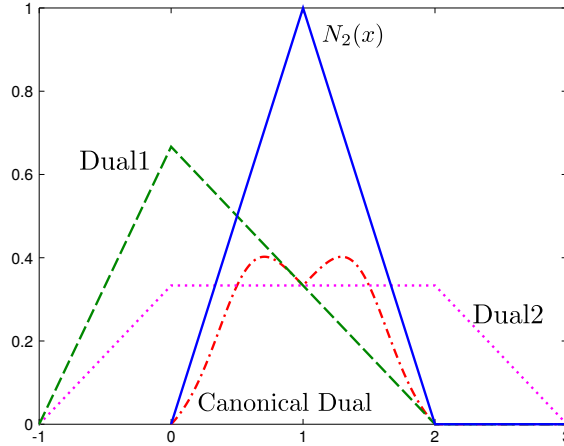


Figure 2: B-spline of order 2 (solid line) and dual windows created by applying Eqs. (7) and (8) for $a = 1$ and $b = \frac{1}{3}$. The dual windows are depicted using the dashed and dotted lines, respectively. Additionally the canonical dual window (dash-dotted line) is depicted.

4. Practical Aspects

For practical application and implementation two points besides the construction of the frame have to be considered: a) The restriction to a finite interval, and b) sampling and the efficient calculation of the expansion coefficients.

4.1. Restriction to Finite Intervals

For a practical implementation it will be necessary to restrict the area of interest and thus the target function $f(x)$ to a finite interval, e.g. $[0, L]$. This can be done either by assuming $f(x)$ to be periodic with period L or by “ignoring” all values of $f(x)$ outside $[0, L]$. In signal processing periodization of the signal and the generating window is a standard option [33], however, for solutions of BEM or FEM problems, that are defined on finite patches and that are, in general, not periodic, this is sub optimal. In these cases periodization may lead to unwanted discontinuities at 0 and L which can result in a high number of “necessary” frame elements around the interval boundaries. “Necessary” in this context means that in the representation many coefficients for frames located around the boundaries will have large absolute values, thus prohibiting an efficient expansion. However, setting all entries of $f(x)$ outside the interval of interest to zero also results in discontinuities at the interval boundaries, which per se are not a problem for the frame used in the expansion, but for the multiplication with the dual frame. One way of dealing with this problem is to expand the interval of interest slightly so that it fully covers the support of the dual frame elements necessary for calculating the frame coefficients. An example: Suppose the function $f(x)$ should be represented in the interval $[0, 3]$ by using frames based on the B-spline of order 2 (the solid line in Fig. 2). To fully cover the interval 4 shifted windows $N_2(x - n)$ with $n \in \{-1, 0, 1, 2\}$ are needed. To calculate the frame coefficients using the dual frames the same amount of shifts of the dual window, which may have a bigger support (e.g. the dual window constructed using Theorem 2 has support $[-1, 3]$), is necessary. Thus, for the correct calculation of the frame coefficients $f(x)$ is needed in the larger interval $[-2, 5]$. If the function $f(x)$ is not known there, $f(x)$ should be expanded smoothly to that interval. For the reconstruction only parts of the frame elements inside $[0, 3]$ will be used.

4.2. Sampling

In Section 3 it was assumed that all the frame elements are functions in $L^2(\mathbb{R})$. For numerical computations it is necessary to do some discretization at one point. This can be done in two ways. One way is to work in the function space and discretize the inner product Eq. (4)

$$\langle f, \tilde{g}_i \rangle = \int_{-\infty}^{\infty} f(x) \tilde{g}_i^*(x) dx \approx \sum_{j=1}^n \omega_j f(x_j) \tilde{g}_i^*(x_j), \quad (9)$$

where $\tilde{g}^*(x)$ denotes the conjugate complex of $\tilde{g}(x)$, and x_j and ω_j are the nodes and weights of an appropriate quadrature method [34, 35, 36], which is adapted to oscillating integrals. Since B-splines have finite support, all integrals in Eq. (9) are definite.

Alternatively, one could already look at a discretized frame (cf. [33] for an overview on sampled and periodized frames). In that case all inner products are simple vector products. Also the canonical dual frame can be calculated easily by taking the pseudo inverse of the matrix containing the sampled frame elements. For the discretized frame the number of frame elements will be finite because the number of necessary modulations is usually a function of the interval length, the frame parameter b , and the number of sampling points used. However, for discretized frames the frame parameters, the number of modulations, and the number of sampling points have to be chosen more carefully (cf. [33]).

4.3. Calculation of the expansion coefficients

If the dual frame is known (either as a function or in a discretized version) it is possible to calculate the coefficients $c_i = \langle f, g_i \rangle$ of the expansion $f(x) = \sum_{i=1}^M c_i g_i(x)$ using the inner product of the target function $f(x)$ with the elements of the dual frames. Alternatively, the unknown frame coefficients can be determined finding the least squares solution

$$\min_{\mathbf{c}} \left\| f(x) - \sum_{i=1}^N c_i g_i(x) \right\|^2. \quad (10)$$

In this case there is no need to know any dual frame, and the fact that a frame is used ensures that Eq. 10 has a stable solution. However, finding a solution to Eq. (10) may take some computation time, and because of the redundancy of a frame there will be several possible solutions. Solving Eq. (10) using the pseudoinverse, which is equivalent of using the canonical dual frame, will, in general, not result in the most efficient solution in terms of sparsity. To arrive at an efficient representation methods from the field of compressed sensing should be used [37, 38, 39] e.g. the orthogonal matching pursuit (OMP) algorithm.

4.3.1. Orthogonal Matching Pursuit

The OMP algorithm is a simple greedy algorithm for finding a sparse solution of a least squares problem $\min_{\mathbf{x}} \|\mathbf{A}\mathbf{x} - \mathbf{b}\|^2$. In its most simple form it consists of the following 6 steps:

1. $\mathbf{r} = \mathbf{b}$.
2. Find the right candidate: $k = \operatorname{argmax}|\mathbf{A}^H\mathbf{r}|$.
3. Add the candidate to the list of used frame atoms: $\mathcal{I} = \mathcal{I} \cup \{k\}$.
4. Find $\mathbf{x}_{\mathcal{I}} = \min_{\mathbf{x}} \|\mathbf{A}_{\mathcal{I}}\mathbf{x} - \mathbf{b}\|^2$ where $\mathbf{A}_{\mathcal{I}}$ only contains the columns of \mathbf{A} with indices in \mathcal{I} .
5. Update the residual $\mathbf{r} = \mathbf{A}_{\mathcal{I}}\mathbf{x}_{\mathcal{I}} - \mathbf{b}$.
6. If $\|\mathbf{r}\| > \text{tol}$ jump to step 2.

The last step is sometimes replaced that the procedure is stopped if a certain number of iterations is reached.

In case of a sampled frame each row of the matrix \mathbf{A} contains one sampled frame element, for non-sampled frames the OMP can be adapted to handle functions. In that case the multiplication in Step 2 has to be replaced by a quadrature to solve $\langle f, g_i \rangle$ and the least squares problem has to be solved using the Gram matrix $\mathbf{G}_{ij} = \langle g_i, g_j \rangle, i, j \in \mathcal{I}$ (see Appendix A for more details). Again, the quadrature used should be adapted to oscillating functions, for calculating the Gram matrix it is also possible to use the fact that the B-splines are polynomials and that calculations can be done analytically by partial integration.

In the literature one can find several modifications of the OMP algorithm (cf. [40] for a small overview of some variants), in the numerical experiments below also the performance of a simple block-OMP algorithm will be investigated, where the frame elements corresponding to the n largest entries of $|\mathbf{A}^H\mathbf{r}|$ are chosen as candidates, with n being the *blocksize*. Judging from the experiments below the block-OMP has the advantage that, in general, the algorithm is faster and that it provides better results (cf. Fig. 8). An expansion of the block algorithm to functions instead of vectors is straightforward.

5. Numerical Experiments

As the target function for the numerical experiments the description of the sound field on a sound hard circular cylinder caused a plane wave is used. This setup has the advantage that it can be reduced to a 2D problem, and that an analytic solution is known (cf. [41]):

$$f(\mathbf{x}) = \frac{2}{\pi kr} \sum_{n=0}^{\infty} \epsilon_n (-i)^{(n-1)} \frac{\cos(n\phi)}{H'_n(kr)}, \quad (11)$$

where $\mathbf{x} = re^{i\phi}$, $\epsilon_0 = 1$, $\epsilon_n = 2, n > 0$ and H'_n is the derivative of the Hankel function of order n . The radius of the circle was set to $r = 1$. In Fig. 3 the real part of the target function $f(\mathbf{x})$ for wavenumbers $k = 5$ and $k = 15$ is shown, in both cases the sum in Eq. (11) was truncated after a fixed number of summands or when the norm of vector containing the values of the new summand on the whole circle was below a certain tolerance.

In the following the relative error between the analytic solution given in Eq. (11) and its expansion using a (for simplicity sampled) B-spline frame with window function $N_2(x)$ will be investigated. Of special interest will be the reconstruction error if only a small number of coefficients are used, in the numerical experiments mainly the errors when using 60 and 120 expansion coefficients are investigated. Since frames are used in the reconstruction different errors for different dual frames are expected. The interval of interest was set to $[0, 3]$ and sampled using 601 points. The parameterization of the circle $[0, 2\pi]$ used in the analytic solution was re-scaled to this interval. This has the advantage that the used frame parameters $a = 1$ and $b = \frac{1}{3}$ and the window function do not have to be re-scaled (see also Section 4.1). The setup implies that 4 (shifted) windows are needed to cover the whole range of $[0, 3]$. Although $f(x)$ is periodic, the B-spline window for generating the frame was not periodized. For calculating the frame coefficients using the dual frames, the interval of interest was extended to cover the full combined support of the necessary dual frames.

For reference the relative error between the original function for the wavenumbers $k = 5$ and $k = 15$ and the approximation using the standard B-spline ansatz functions based on the B-spline of order 2 with 61 and 121 basis

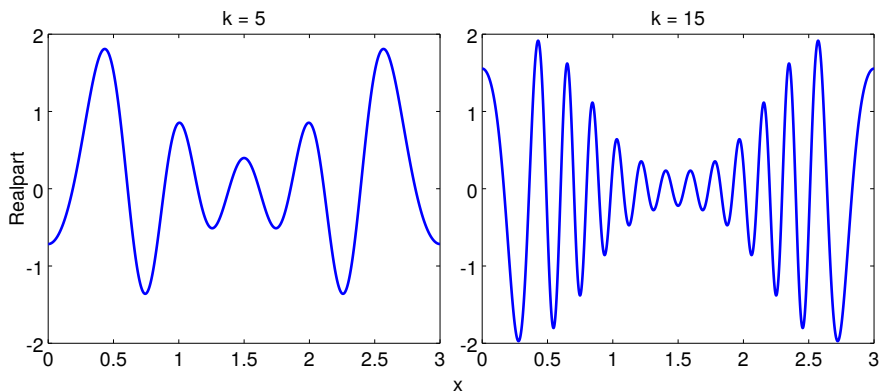


Figure 3: Real part of the solution on the cylinder cross section for $k = 5$ and $k = 15$.

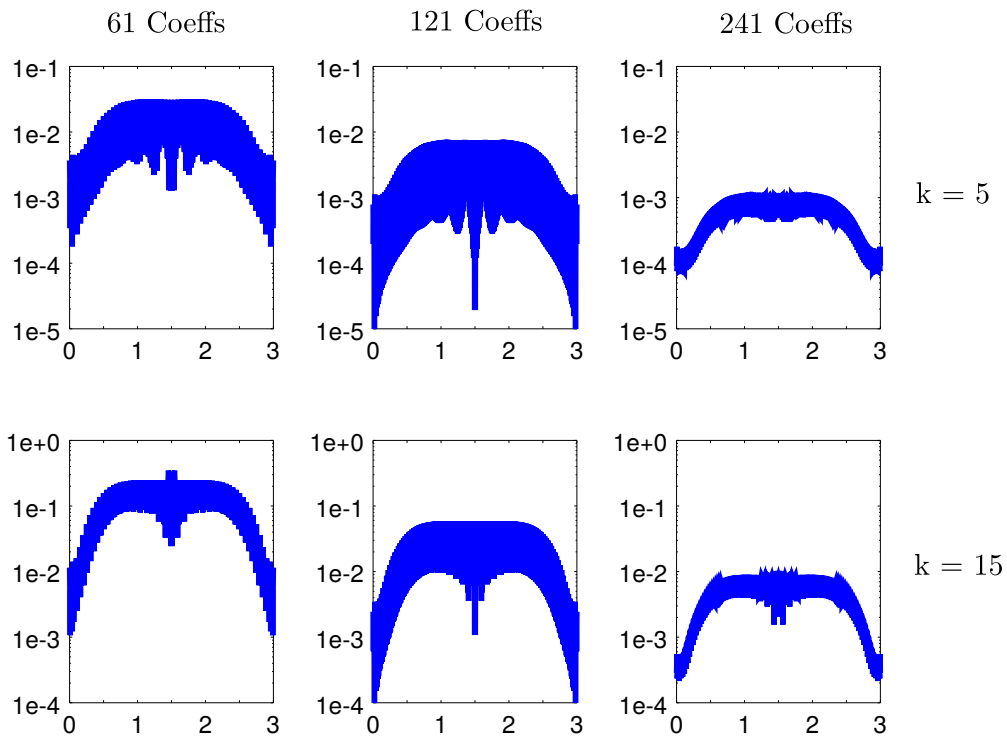


Figure 4: Relative error of the approximation of the target function for the wavenumbers $k = 5$ (upper row) and $k = 15$ (lower row). In the first column the function is expanded into a basis of 61 shifted versions of the scaled B-spline functions of order 2, in the second column the basis consists of 121 shifted version of the B-spline, in the 3rd column 241 basis functions are used.

functions respectively is given in Fig. 4. This is equivalent to discretizing the circle with 60 and 120 elements, and using standard (non-periodic and continuous) linear ansatz functions.

For the numerical experiments with the (vector based) OMP method a slightly modified version of the matlab code from Stephen Becker¹ was used with three different blocksizes (1,10, and 20, see also Section 4.3.1).

¹<https://de.mathworks.com/matlabcentral/fileexchange/32402-cosamp-and-omp-for-sparse-recovery>, last visited 29.11.2017.

5.1. Wavenumber $k = 5$

In Figs. 5 and 6 the errors of the representation of the total field on the cylinder are given. In the different subfigures the coefficients used in the expansion are calculated in 4 different ways. For the graph in the upper left the coefficients are calculated using the dual frame Dual1 defined in Eq. (7), in the upper right the dual frame Dual2 described in Eq. (8) was used, in the lower left the canonical dual frame was used, and in the lower right the coefficients were calculated using the classical OMP algorithm (blocksize = 1). In Fig. 5 only the largest 60 coefficients (in absolute value) were used for the representation, in Fig. 6 the largest 120 coefficients.

Compared to the error when using the standard approach with a basis for piecewise linear functions (see Fig. 4) the relative error when using the B-spline frame is relatively high. Only when using the OMP algorithm the errors are roughly in the same range. At a first glance this would point in the direction that at least for small wavenumbers using more shifted versions of the original window has an advantage over modelling the oscillations using modulations of the window function. So does including oscillations in the ansatz functions of a frame pay off for low wavenumbers at all? After a closer look the answer is 'yes'. The redundancy of the frame offer more possibilities for approximating the target function. For example, when changing the search strategy in the OMP algorithm by increasing the blocksize the error can be reduced to a large degree as can be seen when looking at Fig. 8, where the approximation error is depicted for blocksizes of 10 and 20, respectively. If for example a blocksize of 20 is used the relative error can be reduced to a range of 10^{-7} to 10^{-5} .

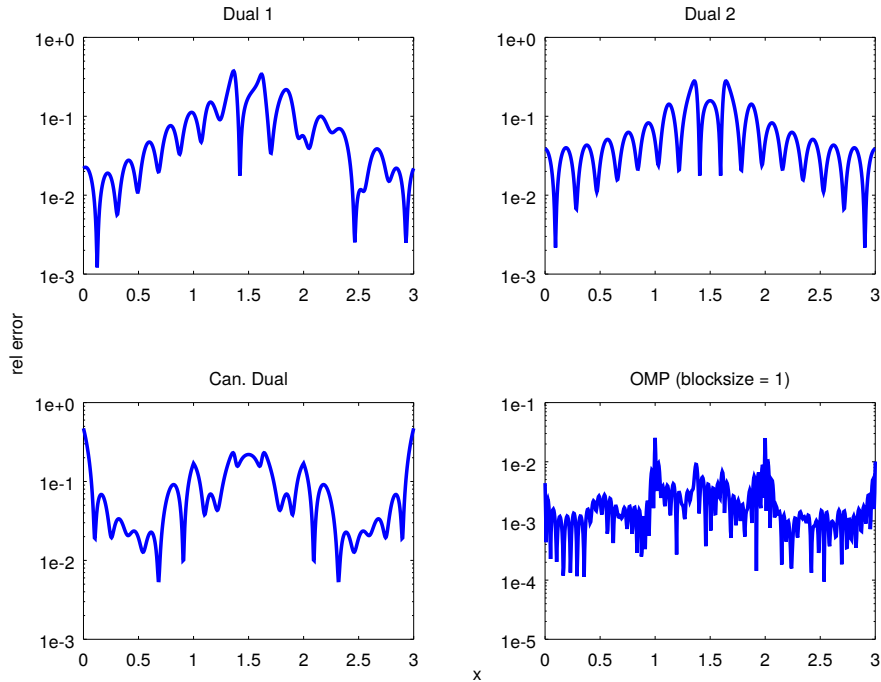


Figure 5: Upper left: Relative approximation error when using the 60 biggest (in absolute value) coefficients using Dual1 (Eq. (7)). Upper right: Approximation error using Dual2 from Eq. (8). Lower left: Canonical dual frame. Lower right: OMP algorithm (blocksize = 1) with 60 iterations. In all cases $k = 5$.

Redundancy in the frame means that there are several ways of approximating the target function, and each representation has its own properties. In Fig. 6 the difference between different dual frames becomes clearly visible. Compared to the canonical dual and Dual1 the error for Dual2 decays very quickly with the number of coefficients used. This can also be seen in Fig. 7 that depicts the absolute value of the coefficients used for a complete reconstruction (relative errors ranging between 10^{-13} and 10^{-15} for the dual frames and 10^{-8} for the OMP with blocksize 1 using 597 coefficients and that was stopped when the absolute error was below a certain tolerance). The coefficients calculated with Dual2 decay very fast for the frame elements associated with a modulation factor bigger then $k = 5$,

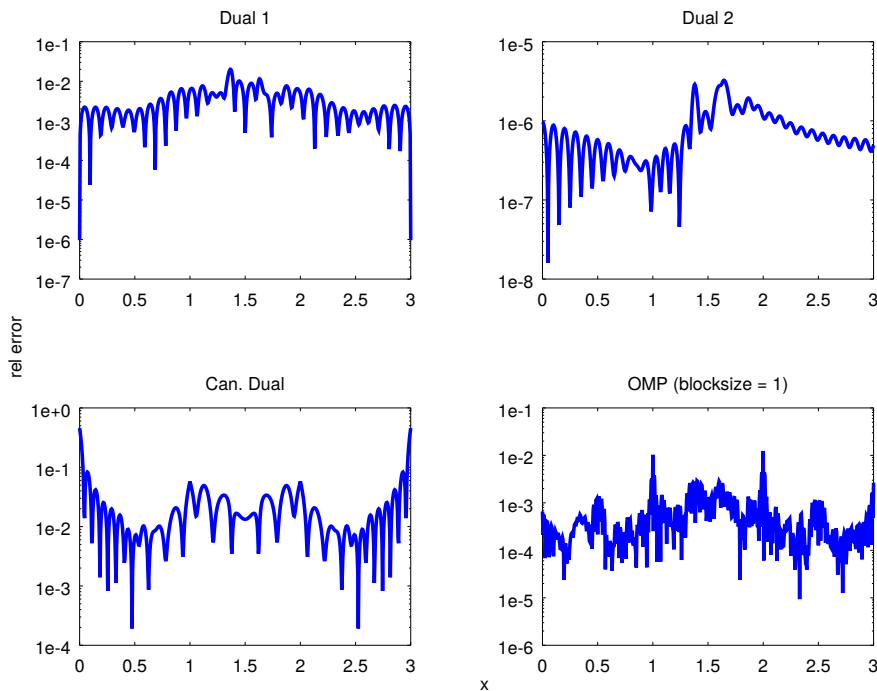


Figure 6: Relative approximation error when using the 120 biggest (in absolute value) coefficients using different dual frames. Upper left: Dual1 defined Eq. (7). Upper right: Dual2 defined in Eq. (8). Lower left: Canonical dual frame. Lower right: Classical OMP algorithm with 120 iterations. In all cases $k = 5$.

while the coefficients in all the other cases decay more slowly. For the canonical dual frame this fact is not so surprising because it can be associated with the pseudoinverse of the matrix containing the sampled frame elements, and it is known that using the pseudoinverse results in a solution that is, in general, not sparse but where the coefficient vector has the smallest ℓ_2 norm. It is more surprising that the OMP algorithm with blocksize 1 that is designed to provide sparse solutions performs that badly compared to Dual2. But again, the performance of the OMP algorithm can be enhanced to a high degree if a blocksize bigger than one is used (see Sec. 4.3.1). It can be seen in Fig. 8 that the performance of the OMP algorithm can be enhanced greatly if the blocksize is raised to 10 or 20, also the algorithm is much faster in these cases, because the cost for solving the small least square problems is small compared all the other calculations involved with the OMP.

To illustrate the advantage of expanding the interval of interest Fig. 9 shows the relative error for the expansion using 120 coefficients calculated with Dual2 *without* expanding the interval of interest. As the OMP does not rely on the dual, the error for the OMP does not change.

5.2. Wavenumber $k = 15$

For higher wavenumbers the block-OMP has a clear advantage when sparse solutions need to be found and the acceptable error tolerance is relatively high. Based on the experience gathered in Section 5.1 the OMP algorithm was used with a blocksize of 20. When looking at the first column in Fig. 10, where only 60 coefficients are used in the expansion, it can be observed that the errors for Dual2 is unacceptable high, the block OMP on the other hand provides an approximation where the maximum relative error is in the range of 10^{-4} to 10^{-2} which may be acceptable for some applications.

In general, the behavior of the coefficients that are calculated using the dual frames is similar as for $k = 5$, however, when looking at Fig. 11 it becomes clear the coefficients start to decay much later. If one looks at the error when using 240 coefficients the “good” behavior of the Dual2 becomes apparent again.

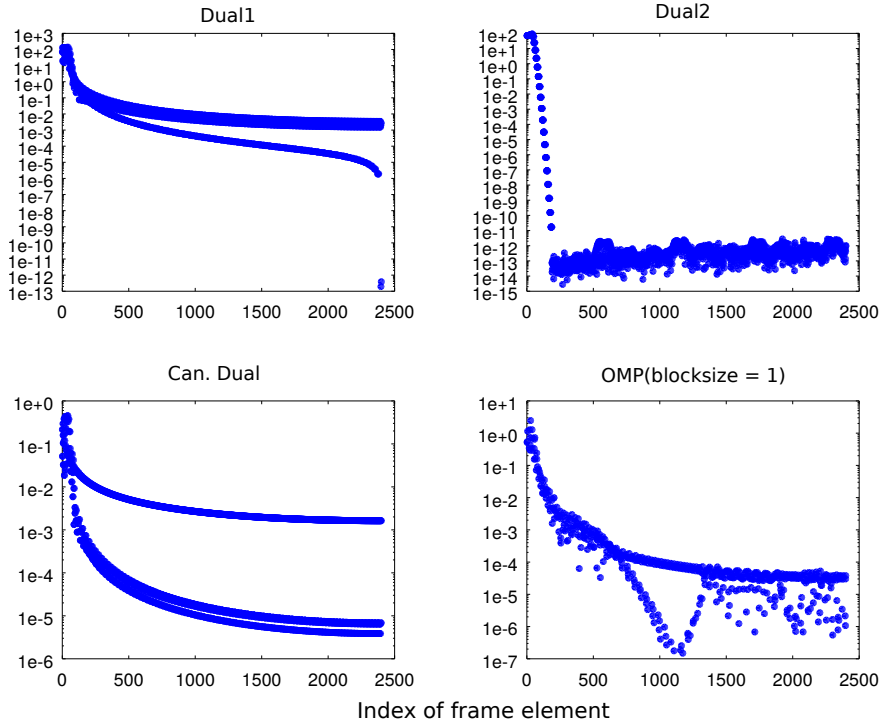


Figure 7: Absolute value of the coefficients used for the expansion of the target function. Upper Left: Coefficients were calculated with Dual1. Upper right: Dual2 was used. Lower left: The canonical dual frame was used. Lower right: 597 coefficients calculated using the classical OMP algorithm (blocksize = 1). Each point in the figure represents one expansion coefficient.

Summary and Outlook

In conclusion, numerical experiments show the potential of Gabor frames for representing solutions of the Helmholtz equation. If B-spline functions are used as generating functions for the Gabor frame, easy ways can be provided to find frame parameters and to construct dual frames, however, there are several ways for finding the expansion coefficients that have different properties. The redundancy of the frame offers several possibilities to construct approximations, and a good way of finding the right frame coefficients need to be found. Using methods like the OMP algorithm have certain advantages if a good strategy of finding the right candidates (see Step 2 in Section 4.3.1) can be developed and implemented. When looking for example at Fig. 12 that contains the zoomed version of Fig. 11 it becomes apparent that the largest coefficients calculated using Dual2 are concentrated around the frame elements with modulations related to the wavenumber. Thus besides using blocksizes bigger than 1, one could in the first few steps concentrate the search for the right candidates to the frame elements with modulations close to the wavenumber of interest, and extend then the search interval to a bigger set of frame elements.

For future work it will also be necessary to look at problems in 3D. On the one hand the extension to 3D is straight forward by using tensor products of one dimensional frames, on the other hand it will be important and necessary to adapt the frames to provide stiffness matrices that can be easily approximated by sparse matrices. To that end it will be necessary to adapt the frames to the Greens function for the Helmholtz equation, and to provide efficient quadrature methods.

Acknowledgments

This study was supported by the Austrian Science Fund (FWF), Project Biotop [I 1018-N25].

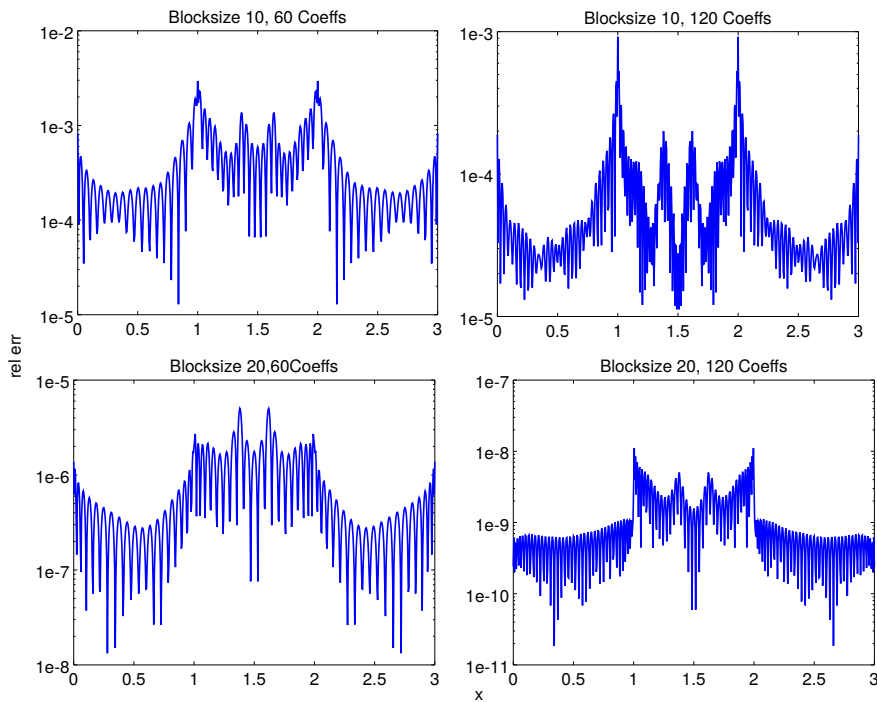


Figure 8: Relative error when the coefficients of the expansion are calculated using the OMP algorithm with different block sizes. Upper half: Blocksize = 10, lower half: Blocksize = 20. On the left 60 coefficients were calculated, on the right side 120. In all cases $k = 5$.

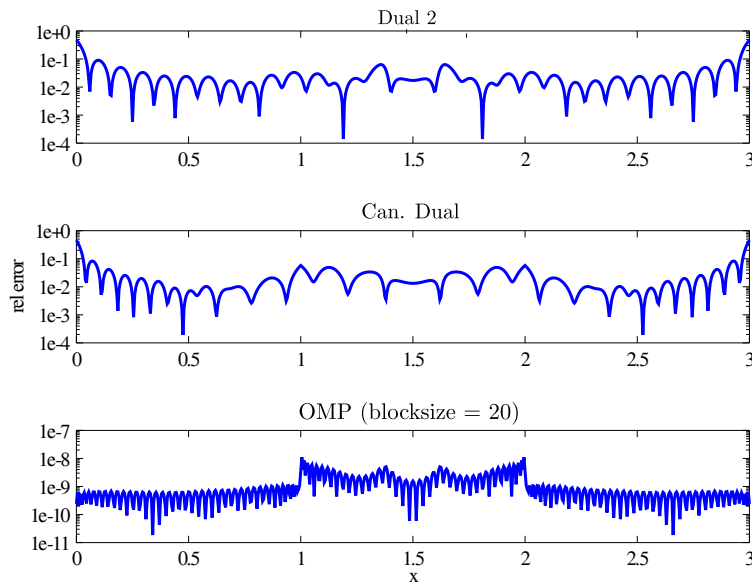


Figure 9: Relative error for the expansion with 120 frame coefficients using Dual2, the canonical dual frame and the OMP algorithm. For the multiplication with the duals the interval of interest was *not* expanded.

Appendix A. OMP for functions

To apply the OMP algorithm to complex valued functions some modifications need to be made in the formulation, which results in a sort of weak formulation:

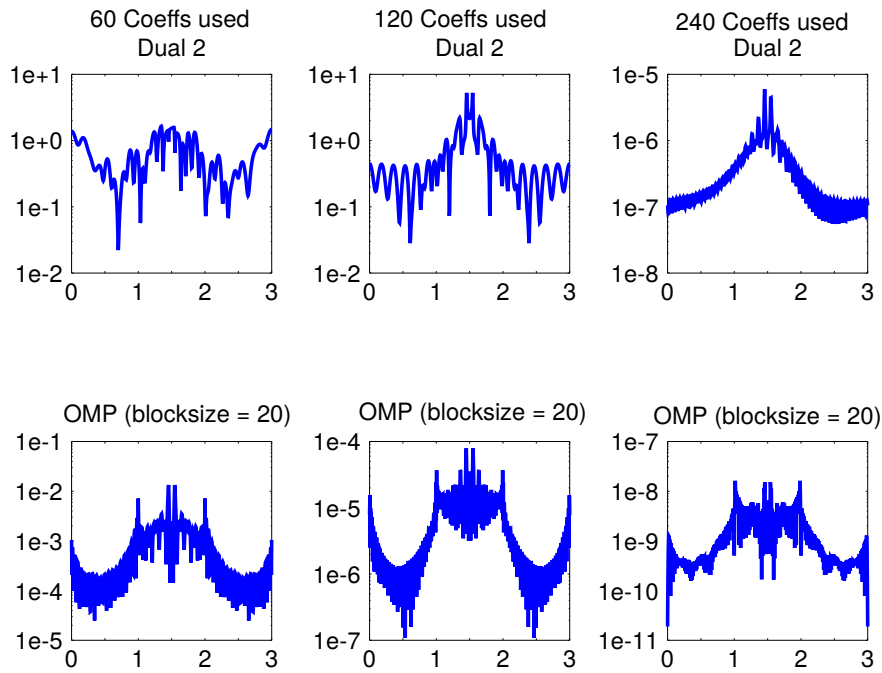


Figure 10: Relative approximation error for the wavenumber $k = 15$ using 60, 120, and 240 coefficients for Dual2 and the OMP with blocksize 20. Upper row: Error for Dual2. Lower row: Error for OMP(20).

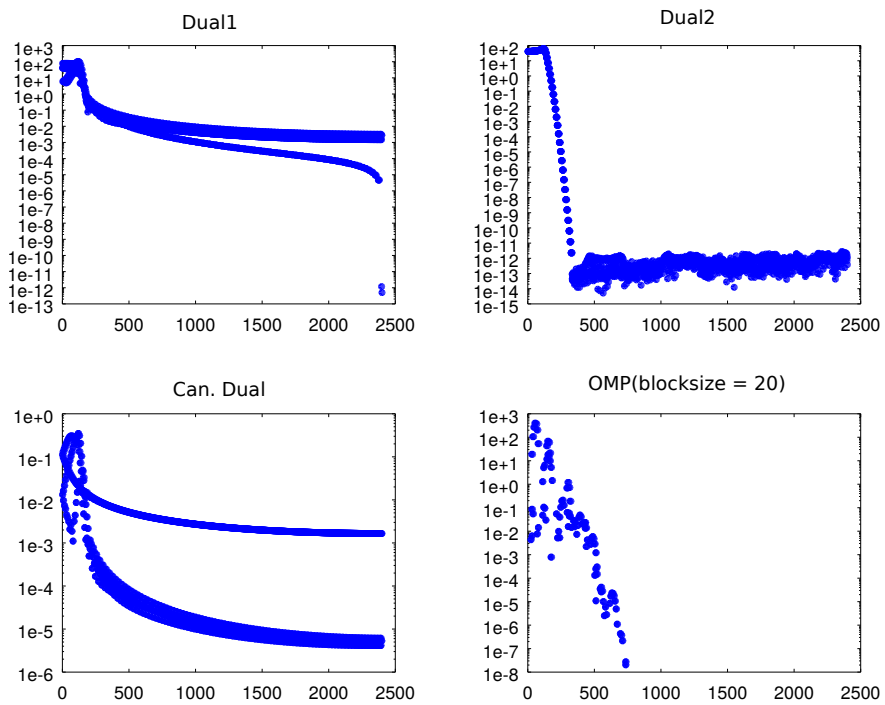


Figure 11: Absolute value of the coefficients for the representation of the target functions. Upper left: Dual1. Upper right: Coefficients are calculated using Dual2. Lower left: Canonical dual. Lower right: OMP with blocksize 20. In all cases the wavenumber was set to $k = 15$.

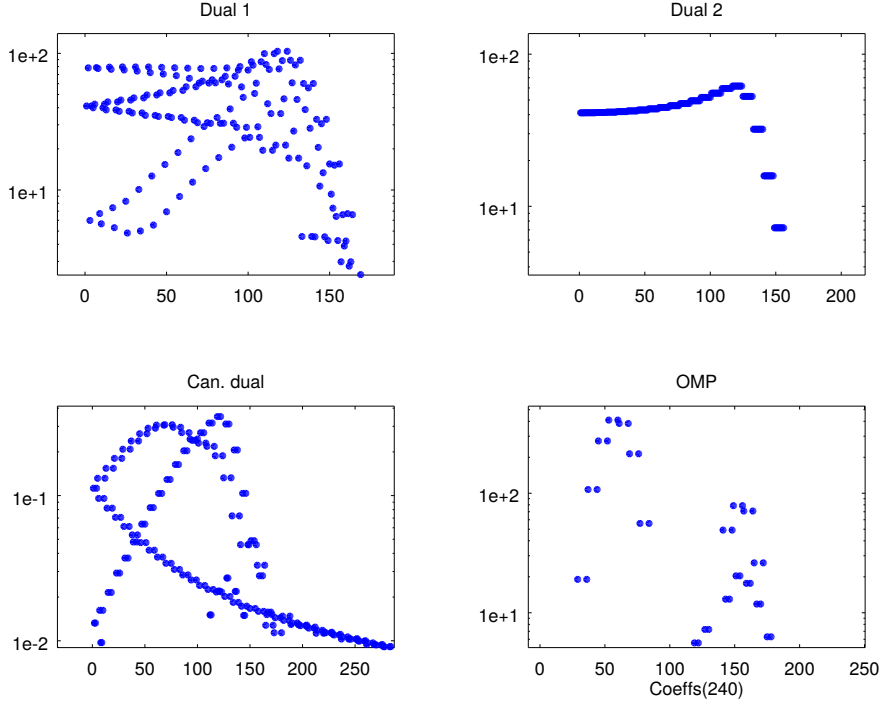


Figure 12: Zoomed version of Fig. 11.

1. $\mathbf{r}'_i = \langle f, g_i \rangle$ for $i = 1, \dots, N$
2. Find the right candidate $k = \operatorname{argmax} |\mathbf{r}'|$
3. Add the candidate to the list of used frame atoms: $\mathcal{I} = \mathcal{I} \cup \{k\}$
4. Find $\gamma = \min_{\mathbf{c}} \|f - \sum_{i \in \mathcal{I}} c_i g_i\|^2$
5. Update $\mathbf{r}'_i = \left\langle \sum_{j \in \mathcal{I}} \gamma_j g_j - f, g_i \right\rangle$
6. If $\|\mathbf{r}'\| > \text{tol}$ jump to step 2

To find the minimum in Step 4

$$\min_{\mathbf{c}} \|f(x) - \sum_{i \in \mathcal{I}} c_i g_i(x)\|^2 = \min_{\mathbf{c}} \left\langle f(x) - \sum_{i \in \mathcal{I}} c_i g_i(x), f(x) - \sum_{i \in \mathcal{I}} c_i g_i(x) \right\rangle \quad (\text{A.1})$$

the vector product is calculated and the derivatives with respect to the real and imaginary part of each c_i need to be set to 0.

The product in Eq. A.1 can be expanded into

$$\langle f, f \rangle - \sum_{i \in \mathcal{I}} \langle f, g_i \rangle c_i^* - \sum_{i \in \mathcal{I}} \langle g_i, f \rangle c_i + \sum_{i, j \in \mathcal{I}} c_i \langle g_i, g_j \rangle c_j^*, \quad (\text{A.2})$$

where c_i^* the conjugate complex of the complex number c_i .

Taking the derivatives with respect to the real and imaginary parts of each $c_i, i \in \mathcal{I}$ results in the two following equations:

$$\sum_{j \in \mathcal{I}} \langle g_i, g_j \rangle c_j^* + \sum_{j \in \mathcal{I}} \langle g_j, g_i \rangle c_j - \langle f, g_i \rangle - \langle g_i, f \rangle = 0, \quad (\text{A.3})$$

$$\sum_{j \in \mathcal{I}} \langle g_i, g_j \rangle c_j^* - \sum_{j \in \mathcal{I}} \langle g_j, g_i \rangle c_j + \langle f, g_i \rangle - \langle g_i, f \rangle = 0, \quad (\text{A.4})$$

which yields the linear system $\mathbf{G}^T \mathbf{c} = \mathbf{f}$ with \mathbf{G}^T being the transpose² of the matrix \mathbf{G} defined by $\mathbf{G}_{ij} = \langle g_i, g_j \rangle$, $\mathbf{f}_i = \langle f, g_i \rangle$, and \mathbf{c} contains the complex valued vector of the unknown coefficients. Please note, that the sizes of \mathbf{G} and \mathbf{f} only depend on the size of the (small) set \mathcal{I} .

References

- [1] L. Gaul, M. Kögl, M. Wagner, *Boundary Element Methods for Engineers and Scientists, An Introductory Course with Advanced Topics*, Springer, 2003.
- [2] M. Fischer, U. Gauger, L. Gaul, A multipole Galerkin boundary element method for acoustics, *Eng. Anal. Boundary Elem.* 28 (2004) 155–162.
- [3] S. Sauter, S. Schwab, *Boundary Element Methods*, Springer, Berlin, 2011.
- [4] Z.-S. Chen, H. Waubke, W. Kreuzer, A formulation of the fast multipole boundary element method (FMBEM) for acoustic radiation and scattering from three-dimensional structures, *J. Comput. Acoust.* 16 (2008) 303–320.
- [5] S. Marburg, Six boundary elements per wavelength. Is that enough?, *J. Comput. Acoust.* 10 (2002) 25–51.
- [6] P. Langer, M. Maeder, C. Guist, M. Krause, S. Marburg, More than six elements per wavelength: The practical use of structural finite element models and their accuracy in comparison with experimental results, *J. Comput. Acoust.* 25 (4) (2017) 1750025.
- [7] O. P. Bruno, C. A. Geuzaine, An $O(1)$ integration scheme for three-dimensional surface scattering problems, *J. Comput. Appl. Math.* 204 (2007) 463–476.
- [8] S. N. Chandler-Wilde, I. G. Graham, S. Langdon, E. A. Spence, Numerical-asymptotic boundary integral methods in high-frequency acoustic scattering, *Acta Numer.* 21 (2012) 89–305.
- [9] H. Feichtinger, T. Strohmer (Eds.), *Gabor Analysis and Algorithms*, Birkhäuser, Boston, 1998.
- [10] K. Gröchenig, *Foundations of Time-Frequency Analysis (Applied and Numerical Harmonic Analysis)*, Birkhäuser, Boston, 2001.
- [11] O. Christensen, *An Introduction to Frames and Riesz Bases*, Birkhäuser, Boston, 2003.
- [12] O. Christensen, *Frames and Bases. An Introductory Course*, Birkhäuser, Boston, 2008.
- [13] J. Kovačević, A. Chebira, Life beyond bases: The advent of frames (part I), *IEEE Signal Process. Mag* 24 (4) (2007) 86–104.
- [14] J. Kovačević, A. Chebira, Life beyond bases: The advent of frames (part II), *IEEE Signal Process. Mag* 24 (5) (2007) 115–125.
- [15] H. Bölcskei, F. Hlawatsch, H. Feichtinger, Frame-theoretic analysis of oversampled filter banks, *IEEE Trans. Signal Processing* 46 (12) (1998) 3256–3268.
- [16] P. Balazs, M. Dörfler, M. Kowalski, B. Torrèsani, Adapted and adaptive linear time-frequency representations: A synthesis point of view, *IEEE Signal Process. Mag.* (special issue: Time-Frequency Analysis and Applications) 30 (2013) 20–31.
- [17] P. Balazs, B. Laback, G. Eckel, W. Deutsch, Time-frequency sparsity by removing perceptually irrelevant components using a simple model of simultaneous masking, *IEEE Trans. Audio, Speech and Language Process.* 18/1 (2010) 34–49.
URL <http://www.kfs.oeaw.ac.at/xxl/mask/mask.pdf>
- [18] P. Balazs, N. Holighaus, T. Necciarì, D. Stoeva, Frame theory for signal processing in psychoacoustics, in: *Excursions in Harmonic Analysis Vol. 5. The February Fourier Talks at the Norbert Wiener Center*, Springer, Basel, 2017, pp. 225–268.
URL <https://arxiv.org/abs/1611.00966>
- [19] R. Stevenson, Adaptive solution of operator equations using wavelet frames, *SIAM J. Numer. Anal.* 41 (3).
- [20] S. Dahlke, M. Fornasier, T. Raasch, Adaptive frame methods for elliptic operator equations, *Adv. Comput. Math.* 27 (1) (2007) 27–63.
- [21] S. Dahlke, M. Fornasier, T. Raasch, R. Stevenson, M. Werner, Adaptive frame methods for elliptic operator equations: The steepest descent approach, *IMA J. Numer. Anal.* 27 (4) (2007) 717–740.
- [22] P. Balazs, Matrix-representation of operators using frames, *Sampl. Theory Signal Image Process.* 7 (1) (2008) 39–54.
- [23] H. Harbrecht, R. Schneider, C. Schwab, Multilevel frames for sparse tensor product spaces, *Numer. Math* 110 (2) (2008) 199–220.
- [24] D. Colton, R. Kress, *Inverse Acoustic and Electromagnetic Scattering Theory* (3rd ed.), Springer, New York, Heidelberg, Dordrecht, London, 2013, Ch. 3.5.
- [25] T. Huges, A. Reali, G. Sangalli, Efficient quadrature for NURBS-based isogeometric analysis, *Comput. Methods Appl. Mech. Eng.* 199 (2010) 301–313.
- [26] J. Dölz, H. Harbrecht, S. Kurz, S. Schöps, F. Wolf, A fast isogeometric BEM for the three dimensional Laplace- and Helmholtz problems, *Comput. Methods Appl. Mech. Eng.* 330 (1) (2018) 83–101.
- [27] C. de Boor, *A Practical Guide to Splines*, Springer, New York, 1987.
- [28] R. Bartels, J. Beatty, B. Barsky, *An Introduction to Splines for Use in Computer Graphics*, Morgan Kaufmann Publishers Inc., San Francisco, 1986.
- [29] L. Piegl, W. Tiller, *The NURBS Book* (2nd ed.), Springer, Berlin, 1997.
- [30] N. Perraudin, N. Holighaus, P. Søndergaard, P. Balazs, Gabor dual windows using convex optimization, in: *Proceedings of the SampTA 2013*, Bremen, Germany, 2013, pp. 33–36.
- [31] T. Strohmer, Numerical algorithms for discrete gabor expansions, in: H. Feichtinger, T. Strohmer (Eds.), *Gabor Analysis and Algorithms, Applied and Numerical Harmonic Analysis*, Birkhäuser, Boston, Basel, Berlin, 1998, Ch. 8.
- [32] O. Christensen, B-spline generated frames, in: B. Foster, P. Massopust (Eds.), *Four Short Courses on Harmonic Analysis., Wavelets, Frames, Time-Frequency Methods, and Applications to Signal and Image Analysis*, Birkhäuser, Bosten, 2010.
- [33] P. L. Søndergaard, Gabor frames by sampling and periodization, *Adv. Comput. Math.* 27 (4) (2007) 355–373.
- [34] G. Evans, Two robust methods for irregular oscillatory integrals over a finite range, *Appl. Num. Math.* 14 (1994) 383–395.

²Please note, that it is really just the transpose, and not the conjugate transpose.

- [35] V. Domínguez, I. Graham, T. Kim, Filon-Clenshaw-Curtis rules for highly-oscillatory integrals with algebraic singularities and stationary points, *SIAM J. Numer. Anal.* (2013) 1542–1566.
- [36] V. Domínguez, Filon-Clenshaw-Curtis rules for a class of highly-oscillatory integrals with logarithmic singularities, *J. Comput. Appl. Math.* 261 (2014) 299–329.
- [37] D. Needell, J. Tropp, CoSaMP: Iterative signal recovery from incomplete and inaccurate samples, *Appl. Comp. Harm. Anal.* 26 (3).
- [38] T. Cai, L. Wang, Orthogonal matching pursuit for sparse signal recovery with noise, *IEEE Trans. Inf. Theory* (2011) 4680–4688.
- [39] Y. Eldar, G. Kutyniok (Eds.), *Compressed Sensing. Theory and Applications*, Cambridge University Press, Cambridge, 2012.
- [40] T. Blumensath, M. Davies, G. Rilling, Greedy algorithms for compressed sensing, in: Y. Eldar, G. Kutyniok (Eds.), *Compressed Sensing. Theory and Applications*, Cambridge University Press, Cambridge, 2012.
- [41] Z.-S. Chen, H. Waubke, A formulation of the boundary element method for acoustic radiation and scattering from two-dimensional structures, *J. Comput. Acoust.* 15 (2007) 333–352.